

Osteoarthritis animal models for biomaterial-assisted osteochondral regeneration

Yi Wang^{1,#}, Yangyang Chen^{2,#}, Yulong Wei^{2,*}

Key Words:

animal model; biomaterial; osteochondral defect; regeneration

From the Contents

Introduction	264
The Pathogenesis of Osteoarthritis	265
Osteochondral Defect Animal Models	267
Applications of Animal Models in Biomaterial Studies	271
Assessment of Osteochondral Defect Regeneration Outcomes	273
Conclusion	274

ABSTRACT

Clinical therapeutics for the regeneration of osteochondral defects (OCD) in the early stages of osteoarthritis remain an enormous challenge in orthopaedics. For in-depth studies of tissue engineering and regenerative medicine in terms of OCD treatment, the utility of an optimal OCD animal model is crucial for assessing the effects of implanted biomaterials on the repair of damaged osteochondral tissues. Currently, the most frequently used in vivo animal models for OCD regeneration include mice, rats, rabbits, dogs, pigs, goats, sheep, horses and nonhuman primates. However, there is no single “gold standard” animal model to accurately recapitulate human disease in all aspects, thus understanding the benefits and limitations of each animal model is critical for selecting the most suitable one. In this review, we aim to elaborate the complex pathological changes in osteoarthritic joints and to summarise the advantages and limitations of OCD animal models utilised for biomaterial testing along with the methodology of outcome assessment. Furthermore, we review the surgical procedures of OCD creation in different species, and the novel biomaterials that promote OCD regeneration. Above all, it provides a significant reference for selection of an appropriate animal model for use in preclinical in vivo studies of biomaterial-assisted osteochondral regeneration in osteoarthritic joints.

*Corresponding author:

Yulong Wei,
yulongwei@hust.edu.cn.

#Author Equally.

<http://doi.org/10.12336/biomatertransl.2022.04.006>

How to cite this article:

Wang, Y.; Chen, Y.; Wei, Y. Osteoarthritis animal models for biomaterial-assisted osteochondral regeneration. *Biomater Transl.* 2022, 3(4), 264-279.



Introduction

Osteoarthritis (OA) is one of the most widespread chronic joint diseases, mainly characterised by high rates of incidence and disability which creates huge threats to human health as well as heavy socio-economic burdens worldwide.^{1, 2} The clinical symptoms of OA affect the whole spine and peripheral joints, especially the interphalangeal joints of the limbs, as well as the hips and knees that undergo heavy load-bearing.³ Among them, the most affected joint is the knee. The risk of OA occurrence in knee joints correlates closely with age, particularly in older women.⁴

To date, the mechanisms of OA remain incompletely elucidated. Compared to other musculoskeletal diseases, the pathology of OA is more complicated due to its extensive

effects on multiple joint tissues. The intricate histopathological changes including cartilage degeneration, abnormal bone remodelling and synovial inflammation make early diagnosis and treatment difficult.⁵ The articular cartilage, subchondral bone, and the interface between them constitute an anatomical unit, defined as osteochondral tissue, which accounts for the load transfer in the joint during weight-bearing and movement. Osteochondral injuries contribute to OA initiation and development,⁶ generally contributing to the joint pain, deformity and dysfunction generated by traumatic injuries and internal diseases associated with cartilage, subchondral bone or the bone-cartilage interface.⁷ Repairing injured osteochondral tissues in the early stages of OA is a promising method to delay or reverse the OA pathological process, leading to reduced clinical impact of OA.

Animal models for biomaterial-assisted osteochondral repair

Current obstacles to clinical research on naturally-occurring OA lie in the chronic and unpredictable disease course,⁸ the inconsistency between clinical symptoms (e.g. joint pain) and the occurrence of tissue structural changes, as well as the complicated underlying molecular mechanisms.⁹ To overcome the limitations of clinical research, the importance of selecting an appropriate animal model for preclinical *in vivo* studies has been widely recognised. Over past decades, numerous animal models have been established for OA research, among which the osteochondral defect (OCD) model is the most frequently used in biomaterials translational research. From the perspective of histology, articular cartilage possesses poor intrinsic healing capability owing to the lack of blood supply and innervation which makes it difficult to repair damaged osteochondral tissues.¹⁰ Moreover, cartilage and subchondral bone are equipped with completely different microstructures and physiological functions.¹¹ Therefore, effective treatment for OCD patients has long been a problem in the field of OA research. In recent years, tissue engineering and regenerative medicine methods provide a possible option for osteochondral tissue regeneration. Advances in cellular therapies, scaffolds, and hydrogels have been widely applied to OCD regeneration.^{6,12} However, there is a significant preclinical gap that should be bridged between the efficacy of implanted biomaterials and the approaches of clinical therapies.

In this review, we focus on OCD animal models. A systematic literature search was conducted in the databases of PubMed and Web of Science using combinations of the following keywords: animal model, *in vivo*, chondral, osteochondral, cartilage, material, biomaterial, mouse, rat, rabbit, dog, pig, goat, sheep, horse, primate. Publications from before October 2022 were initially filtered based on the title and abstract by two independent reviewers. Conflicting results were discussed and determined after full text review. Literature that met the selection criteria (animal models for biomaterial-assisted osteochondral repair) was included. The purpose is to introduce OA pathogenesis, and summarise the advantages and limitations of OCD models in each species along with the methodology of outcome assessment. Novel applications and newly-developed biomaterials in recent translational research are also reviewed, to provide a comprehensive understanding of biomaterial-assisted osteochondral regeneration for the early treatment of OA.

The Pathogenesis of Osteoarthritis

Typically, OA can be categorised into primary OA and secondary OA.¹³ Primary OA, also termed idiopathic OA, indicates a naturally-occurring condition in human patients due to degenerative changes in their joints. Secondary OA refers to a condition normally related to specific causes or risk

factors resulting in joint OA. These causes are often associated with congenital diseases, calcium deposition, metabolic disorders of the bone, and trauma.^{13,14} At present, research into the pathogenesis of post-traumatic OA has been the most extensive. Although some researchers hold different views on the pathogenesis of OA, this section sums up the main consensus on OA initiation and development.

The aetiology of OA is commonly believed to be generated by an imbalance between the catabolic and anabolic processes of the cartilage, accompanied by inflammation in each joint tissue, ultimately leading to joint dysfunction.¹⁵ The current consensus is that OA is a whole-joint disorder involving cartilage erosion, subchondral bone sclerosis, meniscal lesion, and synovitis (**Figure 1**). These characteristic phenotypes were modestly observed in a validated mouse OA model of destabilisation of the medial meniscus (**Figure 2**). Hyaline articular cartilage is a connective tissue without blood or lymphatic vessels that covers the surface of articulating bone.¹⁶ Two major components have been recognised within it. One is the chondrocyte. The other is the extracellular matrix (ECM) which is composed of collagens (mainly type II), glycosaminoglycans, proteoglycans (predominately aggrecan), water and electrolytes. The ECM is responsible for the overall shape and mechanical properties of cartilage.¹⁷ Articular cartilage has typically been divided into four zones: the superficial zone, the middle zone, the deep zone and the calcified zone, as shown in the diagram of osteochondral structure (**Figure 3A**) and in healthy human osteochondral sections (**Figure 3B**). Each of them has a different ECM composition and chondrocyte orientation.^{17,18} Compared to other zones, calcified cartilage has a special composition of glycosaminoglycans and glycoproteins, and acts as an interface between cartilage and subchondral bone.^{19,20} Subchondral bone refers to the bony component lying distal to calcified cartilage.²¹ It is a stress-bearing structure mainly composed of mineralised type I collagen that plays a complementary role to the articular cartilage.²² The menisci are two fibrocartilaginous crescents connected to the surrounding structures by bony and ligamentous attachments.²³ The main components of the meniscus are water (72%), collagens (22%) and glycosaminoglycans (0.8%). Type I collagen accounts for a significant proportion, and types II–V collagens make up the remaining meniscal collagens.²⁴ These biochemical compositions make it an ideal structure to provide shock absorption during joint movement and improve joint congruity^{23,24}. For healthy people, the synovium comprises two types of synoviocytes, respectively characterised by phenotypic features of fibroblasts and macrophages.^{25,26} The cellular components (e.g. lubricin and hyaluronic acid) of synovium are the main source of synovial fluid, contributing to the reduction of friction and the integrity of articular cartilage.²⁶

1 Department of Radiology, Zhongnan Hospital of Wuhan University, Wuhan, Hubei Province, China; 2 Department of Orthopaedics, Union Hospital, Tongji Medical College, Huazhong University of Science and Technology, Wuhan, Hubei Province, China.

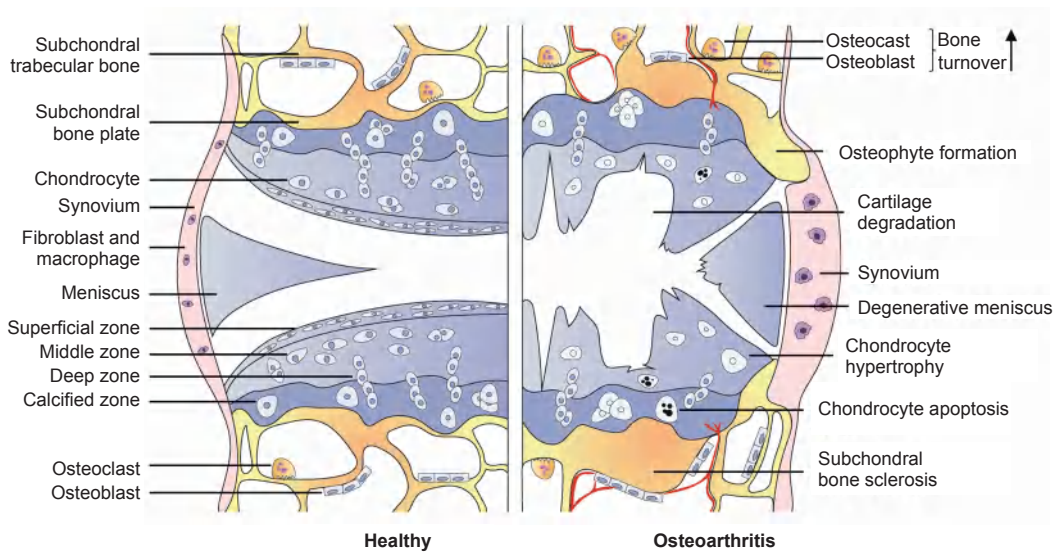


Figure 1. Pathological changes in the development of osteoarthritis.

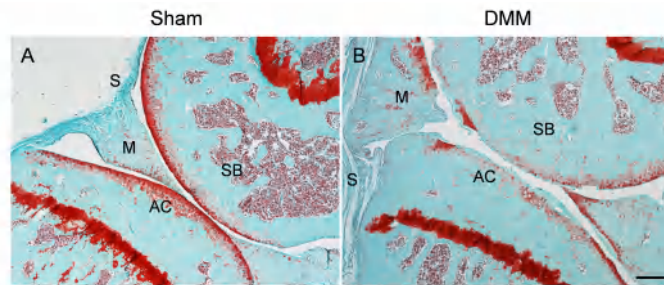


Figure 2. Safranin O and fast green staining of wild-type mouse knee joints at the medial site at 3 months post-sham (A) or post-DMM (B) surgery. DMM surgery was performed by transecting the medial meniscotibial ligament of the knee joint. Sham surgery serves as a control with the meniscotibial ligament intact. Scale bar: 200 μ m. AC: articular cartilage; DMM: destabilisation of the medial meniscus; M: meniscus; S: synovium; SB: subchondral bone.

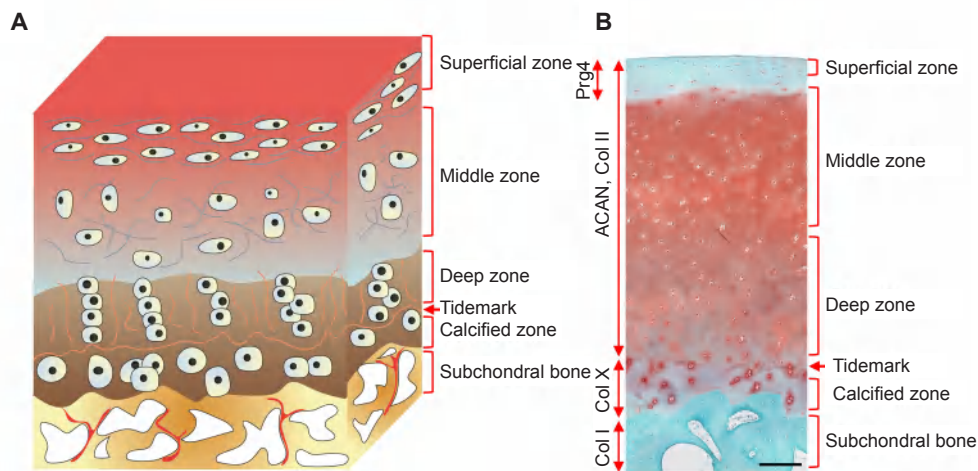


Figure 3. A schematic diagram and representative histological image of an osteochondral unit. (A) The zonal structure of the osteochondral unit. (B) Safranin O and fast green staining of a healthy full-thickness osteochondral unit from an adult human. Scale bar: 200 μ m. ACAN: aggrecan; Col I: type I collagen; Col II: type II collagen; Col X: type X collagen; Prg4: proteoglycan 4.

Animal models for biomaterial-assisted osteochondral repair

Osteoarthritis pathogenesis: cartilage and subchondral bone

During the development of OA, cartilage homeostasis is disrupted and chondrocytes are activated, a period which is characterised by increases in cell proliferation and the production of ECM-degrading enzymes.²⁷ The most intensively-researched ECM-degrading enzymes are matrix metalloproteinase (MMP) family proteins and aggrecanases, both of which degrade native collagens and aggrecan, eventually leading to cartilage damage.^{28, 29} Following the breakdown of ECM, the subchondral bone undergoes abnormal remodelling, and invades through the interface between the bone and calcified cartilage, leading to direct exposure to the joint cavity. Subsequent structural changes of the subchondral bone can be observed in OA, including increased bone turnover, vascular infiltration, and the generation of microfractures, reflected in the clinical symptoms of bone sclerosis, osteophytes and bone cysts.³⁰ The vascular endothelial growth factor released by chondrocytes in the joint is a mediator of angiogenesis. The overexpression of vascular endothelial growth factors and correlated down-regulation of anti-angiogenic factors in OA cartilage may promote the invasion of blood vessels and contribute to progression of the disease.³¹ Inflammatory mediators participate in the breakdown of cartilage ECM. Cytokines such as interleukin (IL)-1, IL-4, IL-6 and tumour necrosis factor α are overexpressed in chondrocytes in early osteoarthritic cartilage.^{32, 33} Their increased secretion results in an anomalous chondrocyte phenotype that impairs the synthesis of ECM collagen and proteoglycans. Furthermore, the release of MMP and aggrecanase enzymes (e.g. MMP-1, -3 and -13), as well as degradative enzymes, are also increased, causing destructive impacts on cartilage components.^{34, 35}

Osteoarthritis pathogenesis: synovial tissue

Although synovial inflammation in OA patients is less pronounced, sufficient evidence exists to verify its pathogenic role. Inflammatory signatures in the OA synovium, mainly observed as cellular hyperproliferation, lymphocyte aggregation and increased vascular infiltration, have been identified by histopathological studies.³⁶ The macrophage is the dominant immune cell type in the OA synovium.³⁷ The quantity of activated macrophages within OA synovium is correlated with disease severity and progression.³⁸ Most studies have led to a common belief that macrophages differentiate into two phenotypes, which are generally termed as classically-activated macrophages (M1) and alternatively-activated macrophages (M2).³⁹ Among them, M1 macrophages respond to intracellular danger-associated molecules, consequently secreting proinflammatory cytokines (e.g. IL-1 β , tumour necrosis factor α and transforming growth factor β), and eventually leading to cartilage damage and bone alterations. In comparison, M2 macrophages exhibit anti-inflammatory and tissue-repair profiles.⁴⁰ Moreover, macrophages and related inflammatory cytokines (e.g. IL-6 and tumour necrosis factor α) also participate in the pathogenesis of rheumatoid arthritis.⁴¹

Osteoarthritis pathogenesis: meniscus

Menisci are mainly composed of two cell populations.

Fibrochondrocytes that are surrounded by abundant ECM are the main cell type located in the inner and middle part of the meniscus, while fibroblasts are the dominant cells distributed in the outer parts.^{24, 42} Vascular and nervous elements exist in the periphery of the meniscus, while the middle and inner portions of the meniscus have limited intrinsic healing ability due to the lack of vasculature.²⁴ Recently, an increasing number of studies have revealed that meniscus in OA likely extends beyond mechanical structure damage to encompass biological interactions. One study has shown that lymphocytes and CD68⁺ macrophages are present in the margin of the meniscus in OA patients.⁴³ The matrix-degrading enzymes, joint-injury-associated inflammatory factors, as well as cytokines and chemokines secreted by the meniscus may result in damage to the joint tissue and subsequent OA development.⁴⁴ Furthermore, the exposure of the meniscus to compressive strain leads to an increase in the release of inducible nitric oxide synthase, IL-1 β and nitrate, suggesting crosstalk between meniscal mechanical loading and joint inflammation.⁴⁵

Osteoarthritis pathogenesis: other factors

With the exception of injury-related post-traumatic OA, other factors also affect OA pathogenesis, including age, gender and obesity. Increased levels of inflammatory cytokines and advanced glycation end products released by chondrocytes have been shown to be prevalent in the elderly. In aging individuals, the accumulated advanced glycation end products in the cartilage bind to receptors on the surface of chondrocytes, resulting in the increased secretion of pro-inflammatory cytokines and vascular endothelial growth factor that eventually contribute to articular cartilage degeneration.^{46, 47} Oestrogen-related receptors (ERRs), which function to maintain tissue homeostasis, have been found to be up-regulated in bone and cartilage.^{48, 49} Two members of the ERR family, ERR α and ERR γ , are essential to the pathogenesis of OA. ERR α -mediated cartilage degradation is associated with IL-1 β and MMPs, whereas ERR γ is the other catabolic regulator of OA pathogenesis, acting by directly upregulating MMP-9 expression.^{50, 51} These studies illustrate the potential effect of gender on OA development. Besides, adipokines released by adipose tissue, especially infrapatellar fat, have been confirmed to be correlated to the degeneration of articular cartilage, suggesting that obesity may also accelerate OA development.⁵² Above all, multiple factors, including inflammatory cytokines, MMPs, cell senescence, oestrogen and biomechanical imbalances participate in the pathogenesis of OA, accompanied by a series of subsequent pathologic changes. These findings provide some potential targets for OA treatment and prevention.

Osteochondral Defect Animal Models

Over the past few decades, multiple induced or spontaneous animal models have been designed and applied to study the development or treatment of OA. The spontaneous models include naturally-occurring and genetically-modified disease models, while the induced models refer to animal models in which disease is primarily induced by surgical operation or intra-articular chemical injection.⁵³ The ideal

OCD animal model should mimic the clinical situation, in particular exhibiting similarities of cartilage physiology with human patients. However, there is no single “gold standard” animal model for OA because of its heterogeneity.⁵⁴ Therefore, selecting the optimal animal model for a particular scientific question is an obvious challenge for researchers. Generally, small animal models may be more suitable for basic pathophysiological and pathogenesis studies of the disease process and are regarded as early screening models for therapeutic interventions. Their advantages include relatively low expense, ease of management, and availability of housing. However, the limitations of these models lie in the inconsistency of joint structure and mechanics between these small animals and humans.⁵⁵ In contrast, large animal models are often used to validate research findings prior to conducting human clinical trials due to their anatomic similarities to humans.⁵⁶ Their disadvantages are mainly associated with greater expense, handling difficulties, longer maturity periods, slower disease processes, and ethical considerations.⁵⁴ Both small and large animals have been used for research on OCD regeneration. Small animal models mainly include the mouse, rat and rabbit,⁵⁷ while large animal models include the dog, pig, sheep, goat and horse, as well as nonhuman primates⁵⁸ (Figure 4). Each species of OCD model has its own benefits and limitations, and the selection of an appropriate animal model should take the research purpose and related factors into consideration.

Current commonly-used OCD animal models utilised for *in vivo* studies are generated by surgical manipulations that create a defect in articular cartilage. According to the Outerbridge classification system,⁵⁹ cartilage defects can be categorised as Grade 0 (normal cartilage), Grade I (nearly normal cartilage with softening and swelling), Grade II (partial-thickness defect with surface fissures), Grade III (full-thickness defect with deep fissures that reach subchondral bone), or Grade IV (OCD with subchondral bone exposed) (Figure 5). The method of constructing defects of various grades depends on the joint physiological conditions of different grades species and the purpose of the experiments.

Mouse

Mouse models have the availability of athymic, transgenic, and knockout strains that offer significant benefits for mechanistic *in vivo* studies. Additionally, mice are convenient to purchase, manage, and feed. However, the application of mouse models in cartilage repair studies is limited due to their small joint size and the extremely thin cartilage, which is only 30 μm thick—50 times thinner than humans.⁶⁰ Additionally, skeletal maturity in mice is difficult to judge because their growth plates remain open throughout their lifetime. An average age of about 10 weeks is usually recommended for mice to be used in a study.⁶¹ In general, a defect of 1.0 mm diameter and 2.0 mm depth on the femoral trochlear groove has been used to create a mouse OCD model.⁶²

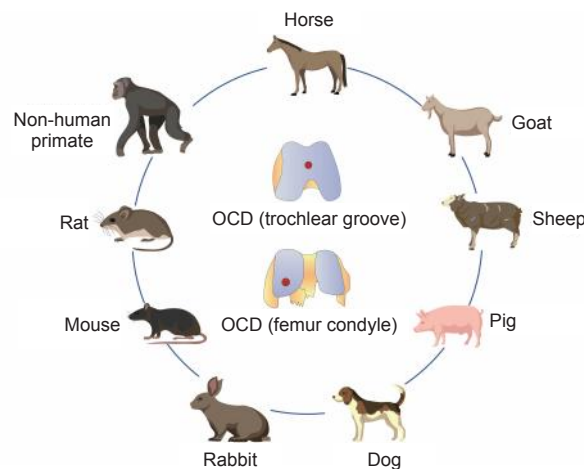


Figure 4. OCD models are created in different animals for tissue engineering studies. OCD: osteochondral defect.

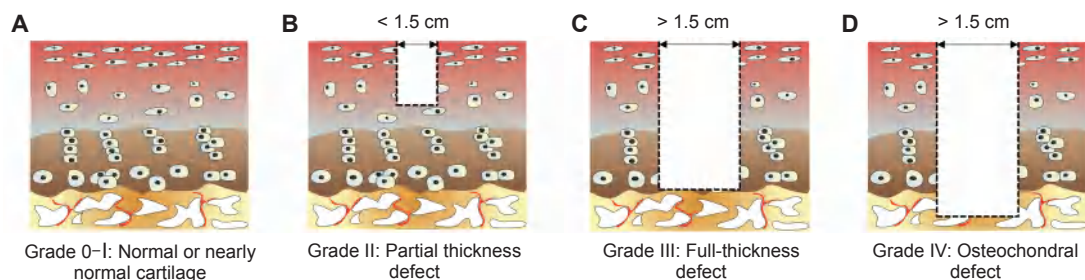


Figure 5. Outerbridge arthroscopic grading system of articular cartilage defects. (A) Grade 0: normal cartilage; Grade I: nearly normal cartilage. (B) Grade II: partial thickness defect. (C) Grade III: full-thickness defect. (D) Grade IV: osteochondral defect.

Animal models for biomaterial-assisted osteochondral repair

Surgical procedure

The OCD model in mice was generated following an established published procedure.⁶³ Briefly, the mice were anaesthetised under sterile conditions. Surgical manipulation was performed under a dissection microscope, and a medial parapatellar incision was made, followed by patella dislocation and exposure of the femoral trochlea. An OCD was then drilled in the middle of the femoral trochlea. The patella was relocated later after the implantation of biomaterials. Finally, the incision was sutured in layers.⁶⁴

Rat

Similar to mice, rat models also have economic advantages, while their larger size makes it feasible to create cartilage defects in biomaterial studies. The thickness of rat articular cartilage is approximately 0.1 mm, which is obviously thicker than mouse cartilage.⁵⁴ Although the body size of rats is larger than mice, their applications are also limited due to their smaller joints and thinner cartilage compared to humans. The growth plate in rats also remains open life-long, which makes it difficult to evaluate skeletal maturity.⁶⁵ Generally, it has been recommended that rats between 9 and 12 weeks should be utilised for biomaterial studies, and the observation period usually lasts 8–12 weeks. The most common approach to creating rat OCD models for assessing biomaterial strategies is to drill a defect (2.0 mm diameter and 2.0 mm deep) on the femoral trochlear groove.

Surgical procedure

In most studies, rats were anaesthetised, and the region of the knees was shaved and sterilised. A medial parapatellar incision was created and the femoral trochlear groove was exposed after patellar dislocation. A defect was drilled at the centre of the trochlear groove. The fragments were washed out with sterile water. After implantation of biomaterials, the patella was relocated, and the incision was closed. Lastly, each rat received a peritoneal injection with the same amount of saline to compensate for fluid loss during the procedure.⁶⁶

Rabbit

Rabbit models have long been used for research on OCD regeneration due to their ease of manipulation, low purchase cost and simple husbandry. Compared to rodent OCD models, the condylar size of mature rabbits is large enough to create defects of 3.0–4.0 mm, which is believed to be an appropriate size for studies of new biomaterial implants. However, significant differences remain in joint biomechanics and gait between humans and rabbits.^{65, 67} Unlike other species and humans, rabbit stifles exhibit an obviously higher flexion angle, and consequently the locations of natural load-bearing are totally different.⁶⁸ In addition, the rabbit meniscus has increased numbers of cells, less vascular infiltration, and improved spontaneous healing capability.^{53, 67} Thus, although the defect size reported in this species is 3.0 mm, larger defects 4.0 or 5.0 mm in diameter are recommended to prevent spontaneous healing.⁶⁵ The thickness of rabbit cartilage is relatively thin, being approximately 0.44 mm at the trochlear groove and 0.3 mm at the anteromedial femoral condyle.⁶⁹

The skeletal maturity age of rabbits is 36 weeks. Rabbits at the age of 8–24 weeks have been utilised in studies. The defects (4.0 mm diameter, 3.0–5.0 mm depth) of OCD rabbit models are commonly created in the femoral trochlea,⁷⁰ as well as the medial⁷¹ and lateral⁷² femoral condyles.

Surgical procedure

Rabbit OCD models were created following the published protocol.⁷⁰ The rabbits were anaesthetised, and their hind limbs were shaved. A parapatellar incision was made to open the joint cavity. Then the patella was dislocated and the femoropatellar groove was exposed. A circular defect was drilled in the femoropatellar groove. Normal saline was used to cool down and remove residual tissues. After the injection of bioactive components, the muscle and wound were sutured separately.

Dog

OCD models have been extensively studied in dogs, which are considered as the closest species to a gold-standard animal model currently available. The anatomic structure of the dog knee joint is very similar to that of the human,⁷³ and this species also suffers from cartilage problems due to the lack of intrinsic healing ability.⁷⁴ In addition, the body size of dogs is large enough to enable arthroscopy and MRI examination. Therefore, dog OCD models utilised for studies of cartilage regeneration may be closer to human conditions compared to rodent or rabbit models. Dogs commonly reach skeletal maturity between 1 and 2 years of age. The cartilage thickness of the femoral condyle (0.95 mm to 1.3 mm) is still thinner than humans. The diameters of defects in OCD models have been reported to be 2–10 mm, with 4 mm being the most commonly used.⁶¹ The defects are generally located in the femoral trochlea,⁷⁵ the medial femoral condyle⁷⁶ or both condyles concurrently.⁷⁴ Although dogs have been considered as a gold standard model for OCD regeneration, the close bond between canines and humans, as well as their status as pets in human households, have emphasised the ethical issues of *in vivo* studies. These concerns have led to efforts to reduce, improve and replace the use of this species as much as possible.

Surgical procedure

Dogs were anaesthetised by intravenous injection and given preoperative antibiotics immediately. The dog was placed in a dorsal recumbent position under sterile conditions. An incision was made on the joint with lateral patellar luxation. The load-bearing areas of the femoral condyles were visualised by adequate joint extension. The defect was often created in the femoral trochlea or the medial femoral condyle. After the implantation of biomaterials, the wound was closed by suturing.⁷⁷

Pig

The joint size, load-bearing conditions, and cartilage thickness of pigs are more similar to humans than dogs or other small animals. Both commercially-raised and miniature pigs have been utilised as models for OA, with the former being widely used for *ex vivo* studies due to the availability of specimens from abattoirs,⁷⁸ while miniature pig strains are more docile and

relatively easy for creating surgical models. Adult mini-pigs have a similar body size and weight to adult humans. Although the joint size of mini-pigs remains smaller than that of humans, defects of 6.0–8.0 mm diameter or larger can be created in the femoral condyles and trochlear grooves. Comparable to humans, the intrinsic healing ability of chondral defects and OCD is also limited in mini-pigs.⁵⁵ Thus, OCD models in pigs should be created in mature individuals to minimise the potential for intrinsic cartilage repair. The pig skeletal maturity age is about 18 months.⁵⁸ Studies have reported that pig cartilage thickness is 1.5 mm,⁷⁹ allowing for the creation of partial or full-thickness cartilage defects in OCD models. However, the construction and management of these specially-bred pigs makes them very expensive. Gotterbarm et al.⁸⁰ have demonstrated that OCDs with a diameter of 6.3 mm do not heal completely in mini-pigs, suggesting the feasibility and utility of this strain for studies of osteochondral regeneration. In general, defects ranging from 6.0 to 8.0 mm in diameter or larger have been created in the trochlear groove,⁸¹ medial femoral condyle,⁸² or both femoral condyles⁸³ for producing pig OCD models. Subsequently, the pig models were followed up for 3–24 months after surgeries.

Surgical procedure

All operations were performed under general anaesthesia. A cylindrical OCD was punched on the patellar groove of the femur while avoiding penetrating the subchondral bone. Biomaterial implants were placed into the defect, and the incision was sutured.⁸¹

Sheep

The sheep is one species which is widely used as an animal model for OCD regeneration since sheep are easy to obtain, convenient to handle, and their maintenance is relatively inexpensive. The anatomy of sheep joints is comparable to that of humans. However, the thickness of sheep cartilage varies significantly between individual subjects, ranging from 0.4 to 1.0 mm, which makes it difficult to analyse and compare different studies using sheep models.⁸⁴ The size of the infrapatellar fat pad in sheep is quite large, thus it requires remarkable flexion to visualise the femoral condyles, which limits the surgical operation. In addition, the generation of sheep OCD commonly involves subchondral bone tissues, which are very hard and dense, bringing out the difficulties of making identical defects when using different manipulations.⁶¹ It has been verified that the critical defect size in sheep is 7.0 mm. Frisbie et al.⁷⁹ and other researchers all acknowledged that the cartilage thickness of the medial femoral condyle is 0.45 mm. In sheep models, the location of created cartilage defects includes the medial femoral condyle,⁸⁵ both femoral condyles,⁸⁶ and the femoral trochlea.⁸⁷ The skeletal maturity age of sheep is around 2–3 years. In general, the OCD sheep model has certain limitations because of their variability in cartilage thickness, relatively large subchondral defects, and later skeletal maturity.

Surgical procedure

An individual sheep was intravenously anaesthetised and placed in dorsal recumbency. The region of the knee was prepared

for disinfection and subsequent surgery. A parapatellar arthrotomy was performed, and the medial and lateral femoral condyles were exposed. OCDs were created in both femoral condyles using a depth-limiting drill guide. Materials were then implanted, and the incision was closed.⁸⁸

Goat

The goat model is widely applied in OCD regeneration, because of their advantages in terms of joint size, the thickness of cartilage and subchondral bone, the feasibility of arthroscopic procedures, and the limited capacity for intrinsic healing. The anatomic structure of goat joints is similar to that of humans, and the size is typically larger than dogs. Since the cartilage thickness of the goat medial femoral condyle has been reported to be between 0.8 and 2.0 mm,⁸⁹ it provides a potential opportunity to study the healing effects of both partial and full-thickness chondral defects. The consistency of goat subchondral bone and the ratio of cartilage to subchondral bone have been reported to be closer to humans compared to small animals, dogs or sheep.^{61,90} Moreover, goat subchondral bone is softer than that of sheep, thus common surgical techniques can be easily used to create OCD models. Meanwhile, goats are relatively inexpensive and more convenient to feed and maintain than other large animals. Goats usually reach skeletal maturity at the age of 2–3 years. The most frequently-used critical defect size in goats is 6.0 mm in diameter.^{89,91} Defects of goat OCD models have been commonly created in the lateral femoral condyles,⁹² medial femoral condyles⁹¹ and trochlear grooves.⁸⁹ In summary, although the size of lesions is still smaller than humans, the goat OCD model could become an accessible large animal model for damaged osteochondral regeneration once the economic limitations can be overcome.

Surgical procedure

A single knee joint was manipulated in each goat. A mini-arthrotomy approach was employed to maintain the integrity of the joint and incision. Minimum exposure of the implantation was maintained by retractors with full extension of the joint, making it possible to gain access to the joint without patellar dislocation. A defect was created on the medial femoral condyle and a biomaterial implant was inserted. In the last step, the knee capsule was closed and skin was sutured.⁹³

Horse

The horse model provides several advantages, listed below, for OCD regeneration studies. Similar to humans, horses also experience cartilage problems including primary and post-traumatic OA.⁵⁴ In addition, the thickness of horse articular cartilage is more similar to humans than any other experimental species. They also have human-like cellular structures, biochemical compositions, and biomechanical characteristics.⁹⁴ Compared to small animal models, the fully-extended and upright stifles in horses during their gaits have the most anatomic similarities to human knees.⁵⁵ It has been reported that the cartilage thickness of horses is approximately 1.75 mm, which is very close to that of humans (2.2 mm).⁷⁹ Furthermore, horse articular cartilage exhibits low intrinsic healing ability. The reported critical defect size in the horse

Animal models for biomaterial-assisted osteochondral repair

is 9.0 mm in diameter, and defects ranging in size from 15 to 20 mm (up to 21 mm) can be created in horse models.^{95, 96} The horse's sizable joint allows for arthroscopic examination, and the comparatively thick cartilage allows for the creation of OCDs that perfectly simulate clinically-relevant-sized defects in human cartilage.⁹⁷ Horses generally achieve skeletal maturity at 2–4 years of age, and at 2–6 years old can be utilised in experimental studies. Commonly, defects 10 mm in diameter and 5.0–10.0 mm in depth have been created in horse OCD models, mainly located in the femoral trochlea,⁹⁸ the medial femoral condyle,⁹⁹ and the lateral trochlear talus.^{100, 101} However, the use of horses for OCD studies requires large facilities, greater technological skills and higher costs. Moreover, horses are companion animals, suggesting that ethical issues should also be considered.

Surgical procedure

The experimental horse was intravenously anaesthetised and positioned in dorsal recumbence. An incision was made at the medial side of the patellar ligaments, then femoropatellar mini-arthrotomy was performed through the wound. OCDs were created by drilling at the centre of the medial femoral trochlear ridge, then the wound was sutured in layers.⁹⁹

Nonhuman primates

Numerous nonhuman primates have been utilised as experimental models in OA studies, including baboons, rhesus monkeys and cynomolgus macaques.^{102, 103} These species exhibit similar genetic, physiological and behavioural characteristics to humans. In addition, the development of naturally-occurring OA involves multiple joints in nonhuman primates, which is very close to the occurrence and progression of spontaneous OA in aging people.^{102, 104} Studies have verified that age-related changes in fertility and reproductive behaviours in several species of female nonhuman primates appear similarities to humans, making it possible to investigate the effects of hormones or reproductive status on the progression of OA.¹⁰⁵ Despite these advantages as an experimental model, nonhuman primates also face limitations related to costs, feasibility, ethical problems and public concerns, which prevent the widespread use of these species.

Surgical procedure

Skeletally-mature cynomolgus macaques were selected to create OCD models. All manipulations were performed under inhalation anaesthesia. A defect (3.2 mm diameter, 4.0 mm depth) was drilled in the load-bearing cartilage surfaces of the medial condyle and the patella. Finally, the wound was closed by suturing, and each animal was given postoperative analgesia.¹⁰⁶

Applications of Animal Models in Biomaterial Studies

Currently, the strategies utilised for OCD treatment can be mainly classified into two categories: non-surgical strategies and surgical strategies, with the former including physical immobilisation and nonsteroidal anti-inflammatory drugs. However, the therapeutic effects of these approaches have

limitations because of the poor intrinsic healing ability of articular cartilage. Therefore, specially-designed structurally and functionally biomimetic tissue-engineered strategies using biomaterials have been established as a promising option for OCD regeneration.¹⁰⁷ Currently, most studies of osteochondral regeneration are still in the preclinical phase, therefore the selection of optimal animal models is important to guarantee successful clinical translation. Small animal models are commonly utilised for primary proof-of-concept studies or degradation and biosafety assessment, prior to validation using large animal models. However, further preclinical biomaterial studies require large animal models based on consideration of the differences in osteochondral healing potential, tissue structures and compositions, as well as technological complexity. The latest applications of OCD animal models for evaluating the repair effects of biomaterials are reviewed in this section.

Mouse osteochondral defect models

Using a full-thickness OCD mouse model, Shen et al.⁶⁴ found that hydroxyapatite-grafted-chitosan implants promoted the remodelling of subchondral bone and the production of osteogenic and chondrogenic factors, resulting in positive effects on osteochondral regeneration. Wesdorp et al.¹⁰⁸ utilised a mouse OCD model to assess the effect of triamcinolone acetonide, an anti-inflammatory drug for cartilage regeneration. The study found that intra-articular injection of triamcinolone acetonide reduces synovial inflammatory levels but negatively affects cartilage repair. Marycz et al.¹⁰⁹ fabricated three-dimensionally (3D)-printed composite of polylactic acid with nano-hydroxyapatite doped with europium (III) ions (nHAp/PLLA@Eu³⁺). Mouse OCD models with a 0.5 mm diameter defect were used to assess its effect on the differentiation of progenitor cells isolated from adipose tissue toward bone and cartilage-forming cells. Study results showed that the established scaffold accelerates osteogenesis and chondrogenesis and has biomedical potential for OCD regeneration.

Rat osteochondral defect models

Mendes et al.¹¹⁰ generated self-assembling tissue intermediates derived from human periosteum-derived stem/progenitor cells, and tissue intermediates were then implanted ectopically into OCDs in rat femoral trochlear grooves. The results showed that tissue intermediates have an intrinsic osteochondral regenerative potential that participates in both subchondral bone and cartilage repair. Li et al.¹¹¹ identified a CD146⁺ subpopulation from adipose-derived mesenchymal stem cells (ADSCs) for cartilage regeneration. The effect of this specific subpopulation on the cartilage microenvironment was assessed by intra-articular injection and scaffold implantation composed of CD146⁺ ADSCs and articular cartilage ECM in rat OCD models. This study has confirmed the role of the CD146⁺ ADSC subpopulation in promoting cartilage repair and emphasised its significance as a potential new treatment. Ji et al.¹¹² designed an immunomodulation-based/porous microsphere composite as a novel controlled drug delivery system. *In vivo* experiments using OCD rat models demonstrated that the

composite structure optimised osteochondral regeneration mediated by macrophage immunomodulation, which may be a potential drug delivery system for cartilage repair. Kim et al.¹¹³ prepared polymeric nanofibrils decorated with cartilage-derived decellularised ECM as a scaffold material for cartilage repair. The repair effect was evaluated by *in vivo* implantation of the ADSC/nanofibril aggregates to the defect located in the rat trochlear groove. The result showed that cartilaginous decellularised ECM-decorated nanofibrils combined with ADSCs have a synergistic effect on improving the cartilage regeneration of OCD.

Rabbit osteochondral defect models

Lin et al.¹¹⁴ successfully constructed a difunctional PEGS/mesoporous bioactive glass (MBG) bilayer scaffold. The effect of the PEGS/MBG scaffold was evaluated using a rabbit OCD model. The results indicated that the scaffold proposed in this study has the potential to be a promising candidate for cartilage and osteochondral regeneration. Yang et al.¹¹⁵ synthesised a novel poly(amino acid) (PAA)-based hydrogel termed PAA-RGD, which they implanted into the defect in a rabbit OCD model. *In vivo* studies demonstrated that the PAA-RGD hydrogel has the potential for OCD regeneration. Qi et al.¹¹⁶ designed a novel oriented-collagen scaffold combined with Wnt5a, which is a growth factor that maintains chondrogenesis. A full-thickness OCD in the rabbit patellar groove was utilised to assess the effect of the Wnt5a/oriented-collagen scaffold. The results showed that the generated scaffold enhanced the regeneration of hyaline cartilage and subchondral bone *in vivo*. Ye et al.¹¹⁷ developed a functionalised self-assembling peptide containing a transforming growth factor β 1-mimetic peptide. A composite scaffold was constructed with a combination of self-assembling peptide and decellularised cartilage ECM, and then implanted into the defect of a rabbit OCD model. *In vivo* studies confirmed appreciable neocartilage restoration. Wu et al.¹¹⁸ used a rabbit OCD model to test the repair effect of a hydrogel implant. They found that the implant as a bioactive supramolecular nanofiber-enabled gelatine methacryloyl hydrogel (BSN-GelMA) effectively achieved seamless osteochondral healing in the gap region of an OCD. Besides studies on cartilage repair, rabbit models have also been utilised for precise diagnosis of OCD. Hong et al.¹¹⁹ exploited a multifunctional nanoprobe based on Fe_3O_4 nanoparticles and self-assembled with kartogenin. An *in vivo* MRI imaging study was performed on a rabbit OCD model. The results showed that the nanoprobe appears distinctively T2-weighted on MR imaging, suggesting it could be applied for disease diagnosis and osteochondral regeneration therapy.

Dog osteochondral defect models

Sun et al.¹²⁰ used a canine OCD model to test a mimetic natural cell-loaded scaffold. The novel scaffold was designed to load allogeneic bone marrow mesenchymal stem cells with the ability to release bone morphogenetic protein 7 in a sustained manner, promoting bone and cartilage regeneration. Baba et al.¹²¹ proposed that the bone marrow stimulation technique augmented by ultra-purified alginate gel induced hyaline-like cartilage repair in a canine OCD model. Onodera et al.¹²²

used canine OCD models to evaluate the therapeutic effect of an acellular technique involving ultra-purified alginate gel implantation. The gel implant significantly enhanced osteochondral repair in canines, especially for small cartilage defects. Ryu et al.¹²³ investigated the efficacy of an implanted biomaterial on the repair of OCD in canine knee cartilage tissues. The 3D-printed biomatrix consisted of human costal-derived cartilage powder, micronised adipose tissue, and fibrin glue. The results showed that the matrix alleviates the inflammatory response and has the potential to repair cartilage. Stefani et al.¹²⁴ developed an acellular agarose hydrogel carrier with embedded dexamethasone-loaded poly(lactic-co-glycolic acid) (PLGA) microspheres. The dexamethasone-loaded osteochondral implant with sustained release was evaluated using a canine OCD model. They demonstrated that a dexamethasone-loaded PLGA microsphere implant plays a role in chondroprotection in the presence of IL-1-induced degradation and improves *in vivo* functional outcomes.

Pig osteochondral defect models

Yan et al.¹²⁵ proposed that PLGA nanoparticles loaded with a hyaluronic acid hydrogel and kartogenin would promote hyaline cartilage and subchondral bone repair in porcine models. Lin et al.¹²⁶ used an OCD in the weight-bearing region of the medial condyle of the pig knee joint to test an implanted acellular spongy PLGA scaffold. The results show that PLGA scaffold implantation combined with treadmill exercise facilitates cartilage regeneration for weight-bearing regions in mini-pigs. Steele et al.¹²⁷ designed a porous zonal microstructure scaffold from a single biocompatible polymer (poly[ϵ -caprolactone]), and evaluated the effect of the scaffold in a porcine OCD model. The scaffold was verified to induce a robust and stable repair in OCD joints. Asen et al.¹²⁸ created an OCD in mini-pigs to demonstrate that implantation of transforming growth factor β 1-releasing scaffolds could improve early-stage cartilage repair *in vivo*. Huang et al.¹²⁹ generated a scaffold composed of lyophilised type II collagen sponge and acellular normal pig subchondral bone, along with natural calcified-zone cartilage, and used the mini-pig OCD model to assess its effect. They found that calcified-zone cartilage plays an important role in osteochondral tissue engineering that mainly repairs hyaline cartilage.

Sheep osteochondral defect models

Bozkurt et al.¹³⁰ created a minimally-invasive tissue-engineering approach, in which specific cartilage proteins were utilised as targets for antibody-coated microspheres. A sheep OCD model was used to verify that implantation of bio-targeted microspheres is an effective therapeutic approach for cartilage defects. Vukasovic et al.¹³¹ demonstrated the efficacy of the established bioreactor-based manufacturing system for cartilage repair by using chronic and acute sheep injury models. Tamaddon et al.¹³² used ten sheep OCD models to evaluate a novel scaffold system consisting of a porous titanium layer and a PLGA-infiltrated collagen layer connected by a porous polylactic acid junction layer. The scaffold exhibited the potential to repair large chondral defects and OCDs in the early stage of OA. Favreau et al.¹³³ utilised a sheep OCD model

Animal models for biomaterial-assisted osteochondral repair

to assess a newly-developed bi-compartmental implant. The implant, comprising therapeutic collagen associated with bone morphogenetic protein 2 and bone marrow mesenchymal stem cell spheroids, was verified to simultaneously regenerate injured articular cartilage and subchondral bone tissues.

Goat osteochondral defect models

Critchley et al.¹³⁴ proposed that a novel bi-phasic, fibre-reinforced cartilaginous template would regenerate the articular cartilage and subchondral bone in caprine joints. Jia et al.¹³⁵ developed a multi-layered scaffold that mimics the structure and components of natural osteochondral tissues. An OCD caprine model was used to evaluate the potential ability of the multi-layered scaffold to repair cartilage. They found that the established multi-layered scaffold significantly improves the biochemical and biomechanical capabilities of the neo-osteochondral tissue. Kon et al.⁹³ created a hemicondylar OCD in goat joint tissues to assess the safety and regenerative properties of a novel hemicondylar aragonite-based scaffold. Burdis et al.¹³⁶ used a 3D-printed polymer framework to guide the self-organisation of early-cartilage microtissues to generate an engineered cartilage implant that mimics native articular cartilage. The caprine OCD model was used to test the effect of this engineered osteochondral implant as a therapeutic strategy for repairing injured synovial joints. Cunniffe et al.¹³⁷ investigated a porous bi-phasic scaffold composed of growth plate ECM and articular cartilage ECM, and verified that the newly-developed scaffold was able to repair OCD in post-implantation caprine joints.

Horse osteochondral defect models

Korthagen et al.¹³⁸ established a bi-layer osteochondral implant composed of a polyetherketoneketone bone anchor and a polyurethane elastomer. The novel implant was confirmed to generate a layer of neocartilage in damaged sites using equine OCD models. Mancini et al.¹³⁹ used an equine model to investigate the potential cartilage repair property of a composite implant that consisted of 3D-printed poly(ϵ -caprolactone) combined with articular cartilage progenitor cells and mesenchymal stromal cells. Murata et al.¹⁴⁰ proposed that the implantation of a scaffold-free 3D-construct of synovial membrane-derived mesenchymal stem cells into an OCD could regenerate the cartilage and subchondral bone in a horse model, suggesting that the technique has potential for the treatment of subchondral bone cysts. Zanotto et al.¹⁴¹ assessed the repair effect of a self-assembling peptide hydrogel combined with trypsin pre-treatment and functionalised with two growth factors (platelet-derived growth factor BB and heparin-binding insulin-like growth factor 1) using a horse OCD model. Results showed that, compared to microfracture alone in a horse model, microfractures combined with trypsin treatment and the functionalised hydrogel improved cartilage repair and integration into surrounding tissues.

Nonhuman primate osteochondral defect models

Park et al.¹⁴² used five skeletally-mature male nonhuman primates (*Cynomolgus* monkey, *Macaca fascicularis*) to create an OCD model, which was utilised to assess the properties of

a novel foetal cartilage-derived progenitor cell-based cartilage gel. Results demonstrated that the foetal cartilage-derived progenitor cell-based cartilage gel exhibits cartilage repair potential and adhesive properties. Jiang et al.¹⁴³ assessed the cartilage repair potential of selected chondrogenic clonal mesenchymal stem cells by implanting them into the defects of cynomolgus monkey OCD models. *In vivo* studies have shown that selected chondrogenic clonal monkey mesenchymal stem cells differentiated into chondrocytes, and the treatment based on selected chondrogenic clonal mesenchymal stem cells enhanced the cartilage repair ability in the cynomolgus monkeys. Ma et al.¹⁴⁴ used a newly-developed 3D clonal mesenchymal stem cell-loaded monkey acellular dermal matrix scaffold to repair injured cartilage in cynomolgus monkeys. Results verified that cartilage defects in monkey models were effectively improved by chondrogenic clonal mesenchymal stem cell treatment.

Assessment of Osteochondral Defect Regeneration Outcomes

To determine whether strategies utilised for OCD regeneration are effective, articular cartilage and subchondral bone repair must be evaluated by various methods including histological, histomorphometric, and biomechanical approaches¹⁴⁵ (Figure 6). The former two assessments are mainly conducted on decalcified and paraffin-embedded joint samples. Generally, histologic assessment adopts different scoring systems to perform gross evaluation and microscopic analysis. These scoring systems range from the simplest, with fewer associated parameters (e.g., Wakitani scores, Pineda scores) to the more complex and integrated ones (e.g., O'driscoll scores, Sellers scores, Forties scores). In addition, International Cartilage Repair Society and Osteoarthritis Research Society International scores are the most widely-utilised systems, with the former often being used for the evaluation of human joints, while the latter is more specific for the assessment of OA staging. Haematoxylin–eosin staining is a basic histological staining technique that is generally employed for the comprehensive evaluation of cells and tissues. However, safranin O/fast green and toluidine blue, as well as alcian blue staining methods are more suitable for evaluating proteoglycan and glycosaminoglycan content. Picrosirius red¹⁴⁶ and Goldner's trichrome¹⁴⁷ are classic techniques used to visualise collagen fibres in histological sections. For undecalcified samples, Stevenel's blue/van Gieson's picrofuchsin dye,¹⁴⁸ toluidine blue¹⁴⁹ and thionine staining are utilised to assess the osteochondral compartment. Histomorphometry mainly measures microtomographic bone-related parameters and quantifies the percentage of biochemical analytes (type I/II/X collagen and/or glycosaminoglycans). The measured bone-related parameters include bone volume/trabecular volume, trabecular number, trabecular separation, trabecular thickness, bone mineral density, mineral apposition rate, and bone formation rate. Parameters such as bone growth, defect volume and osteoid surface area are also frequently used. The assessment of biomechanical properties is usually combined with histological evaluations, which play an important role in regenerative medicine studies, especially osteochondral regeneration. In addition mechanical tests, including

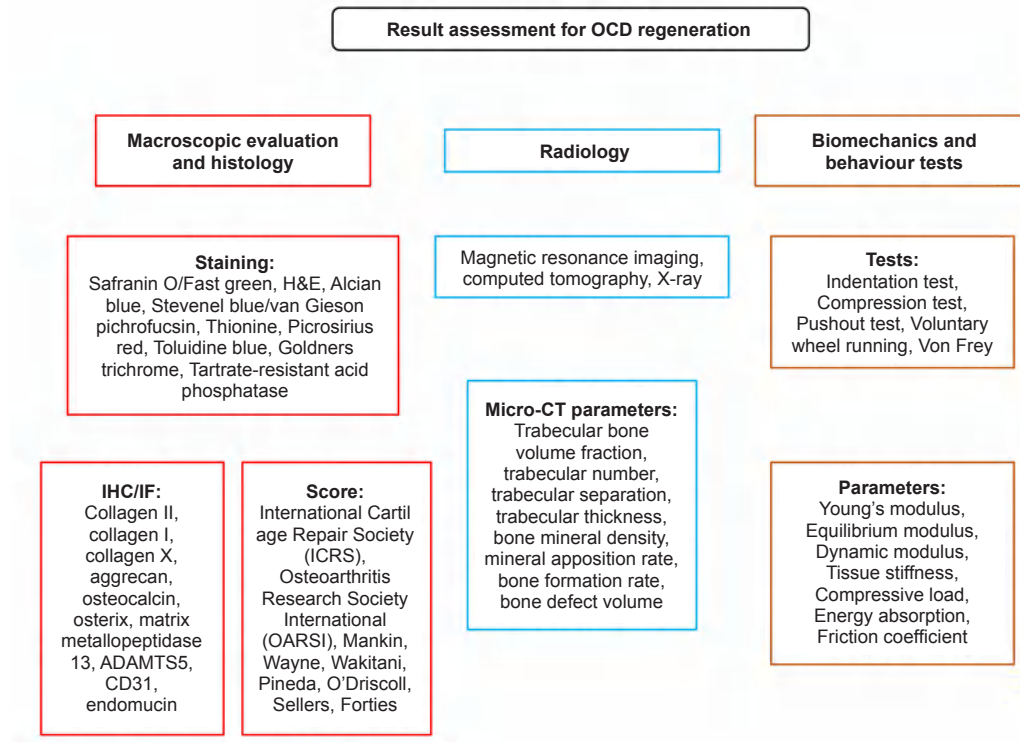


Figure 6. Summary of the evaluation methods for OCD regeneration. ADAMTS5: a disintegrin and metalloproteinase with thrombospondin motif 5; CT: computed tomography; H&E: haematoxylin-eosin; IF: immunofluorescence; IHC: immunohistochemistry; OCD: osteochondral defect.

indentation test, compression test and pushout test, are generally performed on fresh or frozen/thawed samples before histological processing. These biomechanical methods are used to evaluate parameters such as tissue stiffness, compressive load, dynamic modulus, Young's modulus, equilibrium modulus, or contact stress of the cartilage compartment.

Conclusion

Animal translational research plays an important role in exploring the mechanism of specific diseases, improving the methods of early diagnosis, and identifying potential treatment targets. Therefore, the selection of an optimal preclinical animal model is critical to ensure successful translation to the clinical application of biomaterials. There is no single animal model of disease that can perfectly simulate human joint conditions because of the different biomechanics and biokinematics. Although small animal models generally provide benefits regarding availability, feasibility and management, large animal models are more similar to humans, not only physiologically, but also in terms of disease progression. Regardless of the animal chosen, standardised assessment methods in terms of histology, histomorphometry and biomechanics are encouraged in the selection of OCD models. Besides scientific evaluation, practical factors such as ethics, costs and housing need to be considered.

This review presents an overview of current OCD animal models utilised for biomaterial studies along with their advantages and limitations. The pathogenesis of disease progression and scientific assessment of OCD models are also systematically summarised. This study will provide guidance for the selection of an optimal OCD animal model for evaluating biomaterial strategies of osteochondral regeneration.

Author contributions

YWei designed the review. YWang and YC performed the literature research, data extraction and analysis. YWang wrote the manuscript. YWei, YWang, YC revised the manuscript. All authors approved the final version of this manuscript.

Financial support

This work was supported by the National Key R&D Program of China (No. 2021YFA1102600), and the National Natural Science Foundation of China (No. 82002315).

Acknowledgement

None.

Conflicts of interest statement

The authors declare that they have no competing interests.

Open access statement

This is an open access journal, and articles are distributed under the terms of the Creative Commons Attribution-NonCommercial-ShareAlike 4.0 License, which allows others to remix, tweak, and build upon the work non-commercially, as long as appropriate credit is given, and the new creations are licensed under the identical terms.

1. Vina, E. R.; Kwok, C. K. Epidemiology of osteoarthritis: literature update. *Curr Opin Rheumatol.* **2018**, *30*, 160-167.
2. Cross, M.; Smith, E.; Hoy, D.; Nolte, S.; Ackerman, I.; Fransen, M.; Bridgett, L.; Williams, S.; Guillemin, F.; Hill, C. L.; Laslett, L. L.; Jones, G.; Cicuttini, F.; Osborne, R.; Vos, T.; Buchbinder, R.; Woolf, A.; March, L. The global burden of hip and knee osteoarthritis: estimates from the global burden of disease 2010 study. *Ann Rheum Dis.* **2014**, *73*, 1323-1330.
3. Cope, P. J.; Ourradi, K.; Li, Y.; Sharif, M. Models of osteoarthritis: the good, the bad and the promising. *Osteoarthritis Cartilage.* **2019**, *27*, 230-239.
4. Neogi, T. The epidemiology and impact of pain in osteoarthritis. *Osteoarthritis Cartilage.* **2013**, *21*, 1145-1153.
5. Kuyinu, E. L.; Narayanan, G.; Nair, L. S.; Laurencin, C. T. Animal models of osteoarthritis: classification, update, and measurement of outcomes. *J Orthop Surg Res.* **2016**, *11*, 19.
6. Meng, X.; Ziadlou, R.; Grad, S.; Alini, M.; Wen, C.; Lai, Y.; Qin, L.; Zhao, Y.; Wang, X. Animal models of osteochondral defect for testing biomaterials. *Biochem Res Int.* **2020**, 2020, 9659412.
7. Li, X.; Ding, J.; Wang, J.; Zhuang, X.; Chen, X. Biomimetic biphasic scaffolds for osteochondral defect repair. *Regen Biomater.* **2015**, *2*, 221-228.
8. Matthews, G. L. Disease modification: promising targets and impediments to success. *Rheum Dis Clin North Am.* **2013**, *39*, 177-187.
9. Haviv, B.; Bronak, S.; Thein, R. The complexity of pain around the knee in patients with osteoarthritis. *Isr Med Assoc J.* **2013**, *15*, 178-181.
10. Seo, S. S.; Kim, C. W.; Jung, D. W. Management of focal chondral lesion in the knee joint. *Knee Surg Relat Res.* **2011**, *23*, 185-196.
11. Meng, X.; Grad, S.; Wen, C.; Lai, Y.; Alini, M.; Qin, L.; Wang, X. An impaired healing model of osteochondral defect in papain-induced arthritis. *J Orthop Translat.* **2021**, *26*, 101-110.
12. Deng, C.; Chang, J.; Wu, C. Bioactive scaffolds for osteochondral regeneration. *J Orthop Translat.* **2019**, *17*, 15-25.
13. Altman, R.; Asch, E.; Bloch, D.; Bole, G.; Borenstein, D.; Brandt, K.; Christy, W.; Cooke, T. D.; Greenwald, R.; Hochberg, M.; Howell, D.; Kaplan, D.; Koopman, W.; Longley III, S.; Mankin, H.; McShane, D. J.; Medsger, T.; Meenan, R.; Mikkelsen, W.; Moskowitz, R.; Murphy, W.; Rothschild, B.; Segal, M.; Sokoloff, L.; Wolfe, F. Development of criteria for the classification and reporting of osteoarthritis. Classification of osteoarthritis of the knee. Diagnostic and Therapeutic Criteria Committee of the American Rheumatism Association. *Arthritis Rheum.* **1986**, *29*, 1039-1049.
14. Altman, R. D. Criteria for classification of clinical osteoarthritis. *J Rheumatol Suppl.* **1991**, *27*, 10-12.
15. Lambova, S. N.; Müller-Ladner, U. Osteoarthritis - current insights in pathogenesis, diagnosis and treatment. *Curr Rheumatol Rev.* **2018**, *14*, 91-97.
16. Mow, V. C.; Ratcliffe, A.; Poole, A. R. Cartilage and diarthrodial joints as paradigms for hierarchical materials and structures. *Biomaterials.* **1992**, *13*, 67-97.
17. Armiento, A. R.; Stoddart, M. J.; Alini, M.; Eglin, D. Biomaterials for articular cartilage tissue engineering: learning from biology. *Acta Biomater.* **2018**, *65*, 1-20.
18. Pearle, A. D.; Warren, R. F.; Rodeo, S. A. Basic science of articular cartilage and osteoarthritis. *Clin Sports Med.* **2005**, *24*, 1-12.
19. Lyons, T. J.; Stoddart, R. W.; McClure, S. F.; McClure, J. The tidemark of the chondro-osseous junction of the normal human knee joint. *J Mol Histol.* **2005**, *36*, 207-215.
20. Zhang, Y.; Wang, F.; Tan, H.; Chen, G.; Guo, L.; Yang, L. Analysis of the mineral composition of the human calcified cartilage zone. *Int J Med Sci.* **2012**, *9*, 353-360.
21. Madry, H.; van Dijk, C. N.; Mueller-Gerbl, M. The basic science of the subchondral bone. *Knee Surg Sports Traumatol Arthrosc.* **2010**, *18*, 419-433.
22. Pan, J.; Zhou, X.; Li, W.; Novotny, J. E.; Doty, S. B.; Wang, L. In situ measurement of transport between subchondral bone and articular cartilage. *J Orthop Res.* **2009**, *27*, 1347-1352.
23. Englund, M. The role of the meniscus in osteoarthritis genesis. *Rheum Dis Clin North Am.* **2008**, *34*, 573-579.
24. Verdonk, P. C.; Forsyth, R. G.; Wang, J.; Almqvist, K. F.; Verdonk, R.; Veys, E. M.; Verbruggen, G. Characterisation of human knee meniscus cell phenotype. *Osteoarthritis Cartilage.* **2005**, *13*, 548-560.
25. de Sousa, E. B.; Casado, P. L.; Moura Neto, V.; Duarte, M. E.; Aguiar, D. P. Synovial fluid and synovial membrane mesenchymal stem cells: latest discoveries and therapeutic perspectives. *Stem Cell Res Ther.* **2014**, *5*, 112.
26. Scanzello, C. R.; Goldring, S. R. The role of synovitis in osteoarthritis pathogenesis. *Bone.* **2012**, *51*, 249-257.
27. Goldring, M. B.; Marcu, K. B. Cartilage homeostasis in health and rheumatic diseases. *Arthritis Res Ther.* **2009**, *11*, 224.
28. Sandy, J. D. A contentious issue finds some clarity: on the independent and complementary roles of aggrecanase activity and MMP activity in human joint aggrecanolytic. *Osteoarthritis Cartilage.* **2006**, *14*, 95-100.
29. Rengel, Y.; Ospelt, C.; Gay, S. Proteinases in the joint: clinical relevance of proteinases in joint destruction. *Arthritis Res Ther.* **2007**, *9*, 221.
30. Pereira, D.; Ramos, E.; Branco, J. Osteoarthritis. *Acta Med Port.* **2015**, *28*, 99-106.
31. Pfander, D.; Körtje, D.; Zimmermann, R.; Weseloh, G.; Kirsch, T.; Gesslein, M.; Cramer, T.; Swoboda, B. Vascular endothelial growth factor in articular cartilage of healthy and osteoarthritic human knee joints. *Ann Rheum Dis.* **2001**, *60*, 1070-1073.
32. Towle, C. A.; Hung, H. H.; Bonassar, L. J.; Treadwell, B. V.; Mangham, D. C. Detection of interleukin-1 in the cartilage of patients with osteoarthritis: a possible autocrine/paracrine role in pathogenesis. *Osteoarthritis Cartilage.* **1997**, *5*, 293-300.
33. Molnar, V.; Matisić, V.; Kodvanj, I.; Bjelica, R.; Jeleč, Ž.; Hudetz, D.; Rod, E.; Čukelj, F.; Vrdoljak, T.; Vidović, D.; Starešinić, M.; Sabalić, S.; Dobričić, B.; Petrović, T.; Antičević, D.; Borić, I.; Košir, R.; Zmrzljak, U. P.; Primorac, D. Cytokines and chemokines involved in osteoarthritis pathogenesis. *Int J Mol Sci.* **2021**, *22*, 9208.
34. Vincenti, M. P.; Brinckerhoff, C. E. Transcriptional regulation of collagenase (MMP-1, MMP-13) genes in arthritis: integration of complex signaling pathways for the recruitment of gene-specific transcription factors. *Arthritis Res.* **2002**, *4*, 157-164.
35. Mead, T. J.; Apte, S. S. ADAMTS proteins in human disorders. *Matrix Biol.* **2018**, *71-72*, 225-239.
36. Goldenberg, D. L.; Egan, M. S.; Cohen, A. S. Inflammatory synovitis in degenerative joint disease. *J Rheumatol.* **1982**, *9*, 204-209.
37. Wood, M. J.; Leckenby, A.; Reynolds, G.; Spiering, R.; Pratt, A. G.; Rankin, K. S.; Isaacs, J. D.; Haniffa, M. A.; Milling, S.; Hilken, C. M. Macrophage proliferation distinguishes 2 subgroups of knee osteoarthritis patients. *JCI Insight.* **2019**, *4*, e125325.
38. Kraus, V. B.; McDaniel, G.; Huebner, J. L.; Stabler, T. V.; Pieper, C. F.; Shipes, S. W.; Petry, N. A.; Low, P. S.; Shen, J.; McNearney, T. A.; Mitchell, P. Direct in vivo evidence of activated macrophages in human

- osteoarthritis. *Osteoarthritis Cartilage*. **2016**, *24*, 1613-1621.
39. Muraille, E.; Leo, O.; Moser, M. TH1/TH2 paradigm extended: macrophage polarization as an unappreciated pathogen-driven escape mechanism? *Front Immunol*. **2014**, *5*, 603.
 40. Thomson, A.; Hilkens, C. M. U. Synovial macrophages in osteoarthritis: the key to understanding pathogenesis? *Front Immunol*. **2021**, *12*, 678757.
 41. Kurowska-Stolarska, M.; Alivernini, S. Synovial tissue macrophages: friend or foe? *RMD Open*. **2017**, *3*, e000527.
 42. Ghadially, F. N.; Lalonde, J. M.; Wedge, J. H. Ultrastructure of normal and torn menisci of the human knee joint. *J Anat*. **1983**, *136*, 773-791.
 43. Fuhrmann, I. K.; Steinhagen, J.; Rütther, W.; Schumacher, U. Comparative immunohistochemical evaluation of the zonal distribution of extracellular matrix and inflammation markers in human meniscus in osteoarthritis and rheumatoid arthritis. *Acta Histochem*. **2015**, *117*, 243-254.
 44. Favero, M.; Belluzzi, E.; Trisolino, G.; Goldring, M. B.; Goldring, S. R.; Cigolotti, A.; Pozzuoli, A.; Ruggieri, P.; Ramonda, R.; Grigolo, B.; Punzi, L.; Olivotto, E. Inflammatory molecules produced by meniscus and synovium in early and end-stage osteoarthritis: a coculture study. *J Cell Physiol*. **2019**, *234*, 11176-11187.
 45. Gupta, T.; Zielinska, B.; McHenry, J.; Kadmiel, M.; Haut Donahue, T. L. IL-1 and iNOS gene expression and NO synthesis in the superior region of meniscal explants are dependent on the magnitude of compressive strains. *Osteoarthritis Cartilage*. **2008**, *16*, 1213-1219.
 46. DeGroot, J.; Verzijl, N.; Wenting-van Wijk, M. J.; Jacobs, K. M.; Van El, B.; Van Roermund, P. M.; Bank, R. A.; Bijlsma, J. W.; TeKoppele, J. M.; Lafeber, F. P. Accumulation of advanced glycation end products as a molecular mechanism for aging as a risk factor in osteoarthritis. *Arthritis Rheum*. **2004**, *50*, 1207-1215.
 47. Chen, Y. J.; Chan, D. C.; Chiang, C. K.; Wang, C. C.; Yang, T. H.; Lan, K. C.; Chao, S. C.; Tsai, K. S.; Yang, R. S.; Liu, S. H. Advanced glycation end-products induced VEGF production and inflammatory responses in human synoviocytes via RAGE-NF- κ B pathway activation. *J Orthop Res*. **2016**, *34*, 791-800.
 48. Bonnelye, E.; Aubin, J. E. Estrogen receptor-related receptor alpha: a mediator of estrogen response in bone. *J Clin Endocrinol Metab*. **2005**, *90*, 3115-3121.
 49. Bonnelye, E.; Vanacker, J. M.; Dittmar, T.; Begue, A.; Desbiens, X.; Denhardt, D. T.; Aubin, J. E.; Laudet, V.; Fournier, B. The ERR-1 orphan receptor is a transcriptional activator expressed during bone development. *Mol Endocrinol*. **1997**, *11*, 905-916.
 50. Son, Y. O.; Park, S.; Kwak, J. S.; Won, Y.; Choi, W. S.; Rhee, J.; Chun, C. H.; Ryu, J. H.; Kim, D. K.; Choi, H. S.; Chun, J. S. Estrogen-related receptor γ causes osteoarthritis by upregulating extracellular matrix-degrading enzymes. *Nat Commun*. **2017**, *8*, 2133.
 51. Tang, J.; Liu, T.; Wen, X.; Zhou, Z.; Yan, J.; Gao, J.; Zuo, J. Estrogen-related receptors: novel potential regulators of osteoarthritis pathogenesis. *Mol Med*. **2021**, *27*, 5.
 52. Conde, J.; Scotece, M.; Gómez, R.; Lopez, V.; Gómez-Reino, J. J.; Gualillo, O. Adipokines and osteoarthritis: novel molecules involved in the pathogenesis and progression of disease. *Arthritis*. **2011**, *2011*, 203901.
 53. Lampropoulou-Adamidou, K.; Lelovas, P.; Karadimas, E. V.; Liakou, C.; Triantafillopoulos, I. K.; Dontas, I.; Papaioannou, N. A. Useful animal models for the research of osteoarthritis. *Eur J Orthop Surg Traumatol*. **2014**, *24*, 263-271.
 54. McCoy, A. M. Animal models of osteoarthritis: comparisons and key considerations. *Vet Pathol*. **2015**, *52*, 803-818.
 55. Chu, C. R.; Szczodry, M.; Bruno, S. Animal models for cartilage regeneration and repair. *Tissue Eng Part B Rev*. **2010**, *16*, 105-115.
 56. Schneider-Wald, B.; von Thaden, A. K.; Schwarz, M. L. Defect models for the regeneration of articular cartilage in large animals. *Orthopade*. **2013**, *42*, 242-253.
 57. Serra, C. I.; Soler, C. Animal models of osteoarthritis in small mammals. *Vet Clin North Am Exot Anim Pract*. **2019**, *22*, 211-221.
 58. Dias, I. R.; Viegas, C. A.; Carvalho, P. P. Large animal models for osteochondral regeneration. *Adv Exp Med Biol*. **2018**, *1059*, 441-501.
 59. Outerbridge, R. E. The etiology of chondromalacia patellae. *J Bone Joint Surg Br*. **1961**, *43-B*, 752-757.
 60. Glasson, S. S.; Chambers, M. G.; Van Den Berg, W. B.; Little, C. B. The OARSI histopathology initiative - recommendations for histological assessments of osteoarthritis in the mouse. *Osteoarthritis Cartilage*. **2010**, *18 Suppl 3*, S17-23.
 61. Ahern, B. J.; Parvizi, J.; Boston, R.; Schaer, T. P. Preclinical animal models in single site cartilage defect testing: a systematic review. *Osteoarthritis Cartilage*. **2009**, *17*, 705-713.
 62. Wang, P.; Zhang, F.; He, Q.; Wang, J.; Shiu, H. T.; Shu, Y.; Tsang, W. P.; Liang, S.; Zhao, K.; Wan, C. Flavonoid compound icariin activates hypoxia inducible factor-1 α in chondrocytes and promotes articular cartilage repair. *PLoS One*. **2016**, *11*, e0148372.
 63. Eltawil, N. M.; De Bari, C.; Achan, P.; Pitzalis, C.; Dell'accio, F. A novel in vivo murine model of cartilage regeneration. Age and strain-dependent outcome after joint surface injury. *Osteoarthritis Cartilage*. **2009**, *17*, 695-704.
 64. Shen, K.; Liu, X.; Qin, H.; Chai, Y.; Wang, L.; Yu, B. HA-g-CS implant and moderate-intensity exercise stimulate subchondral bone remodeling and promote repair of osteochondral defects in mice. *Int J Med Sci*. **2021**, *18*, 3808-3820.
 65. Cook, J. L.; Hung, C. T.; Kuroki, K.; Stoker, A. M.; Cook, C. R.; Pfeiffer, F. M.; Sherman, S. L.; Stannard, J. P. Animal models of cartilage repair. *Bone Joint Res*. **2014**, *3*, 89-94.
 66. Park, K. S.; Kim, B. J.; Lih, E.; Park, W.; Lee, S. H.; Joung, Y. K.; Han, D. K. Versatile effects of magnesium hydroxide nanoparticles in PLGA scaffold-mediated chondrogenesis. *Acta Biomater*. **2018**, *73*, 204-216.
 67. Gregory, M. H.; Capito, N.; Kuroki, K.; Stoker, A. M.; Cook, J. L.; Sherman, S. L. A review of translational animal models for knee osteoarthritis. *Arthritis*. **2012**, *2012*, 764621.
 68. Proffen, B. L.; McElfresh, M.; Fleming, B. C.; Murray, M. M. A comparative anatomical study of the human knee and six animal species. *Knee*. **2012**, *19*, 493-499.
 69. Räsänen, T.; Messner, K. Regional variations of indentation stiffness and thickness of normal rabbit knee articular cartilage. *J Biomed Mater Res*. **1996**, *31*, 519-524.
 70. Radhakrishnan, J.; Manigandan, A.; Chinnaswamy, P.; Subramanian, A.; Sethuraman, S. Gradient nano-engineered in situ forming composite hydrogel for osteochondral regeneration. *Biomaterials*. **2018**, *162*, 82-98.
 71. Levingstone, T. J.; Thompson, E.; Matsiko, A.; Schepens, A.; Gleeson, J. P.; O'Brien, F. J. Multi-layered collagen-based scaffolds for osteochondral defect repair in rabbits. *Acta Biomater*. **2016**, *32*, 149-160.
 72. Ramallal, M.; Maneiro, E.; López, E.; Fuentes-Boquete, I.; López-Armada, M. J.; Fernández-Sueiro, J. L.; Galdo, F.; De Toro, F. J.; Blanco, F. J. Xenotransplantation of pig chondrocytes into rabbit to treat localized articular cartilage defects: an animal model. *Wound Repair Regen*. **2004**, *12*, 337-345.

Animal models for biomaterial-assisted osteochondral repair

73. Cook, J. L.; Kuroki, K.; Visco, D.; Pelletier, J. P.; Schulz, L.; Lafeber, F. P. The OARSI histopathology initiative - recommendations for histological assessments of osteoarthritis in the dog. *Osteoarthritis Cartilage*. **2010**, *18 Suppl 3*, S66-79.
74. Shortkroff, S.; Barone, L.; Hsu, H. P.; Wrenn, C.; Gagne, T.; Chi, T.; Breinan, H.; Minas, T.; Sledge, C. B.; Tubo, R.; Spector, M. Healing of chondral and osteochondral defects in a canine model: the role of cultured chondrocytes in regeneration of articular cartilage. *Biomaterials*. **1996**, *17*, 147-154.
75. van Dyk, G. E.; DeJardin, L. M.; Flo, G.; Johnson, L. L. Cancellous bone grafting of large osteochondral defects: an experimental study in dogs. *Arthroscopy*. **1998**, *14*, 311-320.
76. Cook, S. D.; Patron, L. P.; Salkeld, S. L.; Rueger, D. C. Repair of articular cartilage defects with osteogenic protein-1 (BMP-7) in dogs. *J Bone Joint Surg Am*. **2003**, *85-A Suppl 3*, 116-123.
77. Kazemi, D.; Shams Asenjan, K.; Dehdilani, N.; Parsa, H. Canine articular cartilage regeneration using mesenchymal stem cells seeded on platelet rich fibrin: macroscopic and histological assessments. *Bone Joint Res*. **2017**, *6*, 98-107.
78. Vernon, L.; Abadin, A.; Wilensky, D.; Huang, C. Y.; Kaplan, L. Subphysiological compressive loading reduces apoptosis following acute impact injury in a porcine cartilage model. *Sports Health*. **2014**, *6*, 81-88.
79. Frisbie, D. D.; Cross, M. W.; McIlwraith, C. W. A comparative study of articular cartilage thickness in the stifle of animal species used in human pre-clinical studies compared to articular cartilage thickness in the human knee. *Vet Comp Orthop Traumatol*. **2006**, *19*, 142-146.
80. Gotterbarm, T.; Breusch, S. J.; Schneider, U.; Jung, M. The minipig model for experimental chondral and osteochondral defect repair in tissue engineering: retrospective analysis of 180 defects. *Lab Anim*. **2008**, *42*, 71-82.
81. Vasara, A. I.; Hyttinen, M. M.; Pulliainen, O.; Lammi, M. J.; Jurvelin, J. S.; Peterson, L.; Lindahl, A.; Helminen, H. J.; Kiviranta, I. Immature porcine knee cartilage lesions show good healing with or without autologous chondrocyte transplantation. *Osteoarthritis Cartilage*. **2006**, *14*, 1066-1074.
82. Hembry, R. M.; Dyce, J.; Driesang, I.; Hunziker, E. B.; Fosang, A. J.; Tyler, J. A.; Murphy, G. Immunolocalization of matrix metalloproteinases in partial-thickness defects in pig articular cartilage. A preliminary report. *J Bone Joint Surg Am*. **2001**, *83*, 826-838.
83. Chang, C. H.; Kuo, T. F.; Lin, C. C.; Chou, C. H.; Chen, K. H.; Lin, F. H.; Liu, H. C. Tissue engineering-based cartilage repair with allogeneic chondrocytes and gelatin-chondroitin-hyaluronan tri-copolymer scaffold: a porcine model assessed at 18, 24, and 36 weeks. *Biomaterials*. **2006**, *27*, 1876-1888.
84. Lu, Y.; Hayashi, K.; Hecht, P.; Fanton, G. S.; Thabit, G.; Cooley, A. J.; Edwards, R. B.; Markel, M. D. The effect of monopolar radiofrequency energy on partial-thickness defects of articular cartilage. *Arthroscopy*. **2000**, *16*, 527-536.
85. Tytherleigh-Strong, G.; Hurtig, M.; Miniaci, A. Intra-articular hyaluronan following autogenous osteochondral grafting of the knee. *Arthroscopy*. **2005**, *21*, 999-1005.
86. Siebert, C. H.; Miltner, O.; Weber, M.; Sopka, S.; Koch, S.; Niedhart, C. Healing of osteochondral grafts in an ovine model under the influence of bFGF. *Arthroscopy*. **2003**, *19*, 182-187.
87. Kandel, R. A.; Grynepas, M.; Pilliar, R.; Lee, J.; Wang, J.; Waldman, S.; Zalzal, P.; Hurtig, M. Repair of osteochondral defects with biphasic cartilage-calcium polyphosphate constructs in a sheep model. *Biomaterials*. **2006**, *27*, 4120-4131.
88. Mohan, N.; Gupta, V.; Sridharan, B. P.; Mellott, A. J.; Easley, J. T.; Palmer, R. H.; Galbraith, R. A.; Key, V. H.; Berklund, C. J.; Detamore, M. S. Microsphere-based gradient implants for osteochondral regeneration: a long-term study in sheep. *Regen Med*. **2015**, *10*, 709-728.
89. Brehm, W.; Aklin, B.; Yamashita, T.; Rieser, F.; Trüb, T.; Jakob, R. P.; Mainil-Varlet, P. Repair of superficial osteochondral defects with an autologous scaffold-free cartilage construct in a caprine model: implantation method and short-term results. *Osteoarthritis Cartilage*. **2006**, *14*, 1214-1226.
90. Jackson, D. W.; Lalor, P. A.; Aberman, H. M.; Simon, T. M. Spontaneous repair of full-thickness defects of articular cartilage in a goat model. A preliminary study. *J Bone Joint Surg Am*. **2001**, *83*, 53-64.
91. Niederauer, G. G.; Slivka, M. A.; Leatherbury, N. C.; Korvick, D. L.; Harroff, H. H.; Ehler, W. C.; Dunn, C. J.; Kieswetter, K. Evaluation of multiphase implants for repair of focal osteochondral defects in goats. *Biomaterials*. **2000**, *21*, 2561-2574.
92. Dell'Accio, F.; Vanlauwe, J.; Bellemans, J.; Neys, J.; De Bari, C.; Luyten, F. P. Expanded phenotypically stable chondrocytes persist in the repair tissue and contribute to cartilage matrix formation and structural integration in a goat model of autologous chondrocyte implantation. *J Orthop Res*. **2003**, *21*, 123-131.
93. Kon, E.; Robinson, D.; Shani, J.; Alves, A.; Di Matteo, B.; Ashmore, K.; De Caro, F.; Dulic, O.; Altschuler, N. Reconstruction of large osteochondral defects using a hemicondylar aragonite-based implant in a caprine model. *Arthroscopy*. **2020**, *36*, 1884-1894.
94. Malda, J.; Benders, K. E.; Klein, T. J.; de Grauw, J. C.; Kik, M. J.; Huttmacher, D. W.; Saris, D. B.; van Weeren, P. R.; Dhert, W. J. Comparative study of depth-dependent characteristics of equine and human osteochondral tissue from the medial and lateral femoral condyles. *Osteoarthritis Cartilage*. **2012**, *20*, 1147-1151.
95. Convery, F. R.; Akeson, W. H.; Keown, G. H. The repair of large osteochondral defects. An experimental study in horses. *Clin Orthop Relat Res*. **1972**, *82*, 253-262.
96. Hidaka, C.; Goodrich, L. R.; Chen, C. T.; Warren, R. F.; Crystal, R. G.; Nixon, A. J. Acceleration of cartilage repair by genetically modified chondrocytes over expressing bone morphogenetic protein-7. *J Orthop Res*. **2003**, *21*, 573-583.
97. Strauss, E. J.; Goodrich, L. R.; Chen, C. T.; Hidaka, C.; Nixon, A. J. Biochemical and biomechanical properties of lesion and adjacent articular cartilage after chondral defect repair in an equine model. *Am J Sports Med*. **2005**, *33*, 1647-1653.
98. Seo, J. P.; Kambayashi, Y.; Itho, M.; Haneda, S.; Yamada, K.; Furuoka, H.; Tabata, Y.; Sasaki, N. Effects of a synovial flap and gelatin/ β -tricalcium phosphate sponges loaded with mesenchymal stem cells, bone morphogenetic protein-2, and platelet rich plasma on equine osteochondral defects. *Res Vet Sci*. **2015**, *101*, 140-143.
99. Vindas Bolaños, R. A.; Cokelaere, S. M.; Estrada McDermott, J. M.; Benders, K. E.; Gbureck, U.; Plomp, S. G.; Weinans, H.; Groll, J.; van Weeren, P. R.; Malda, J. The use of a cartilage decellularized matrix scaffold for the repair of osteochondral defects: the importance of long-term studies in a large animal model. *Osteoarthritis Cartilage*. **2017**, *25*, 413-420.
100. McCarrel, T. M.; Pownder, S. L.; Gilbert, S.; Koff, M. F.; Castiglione, E.; Saska, R. A.; Bradica, G.; Fortier, L. A. Two-year evaluation of osteochondral repair with a novel biphasic graft saturated in bone marrow in an equine model. *Cartilage*. **2017**, *8*, 406-416.
101. Maninchedda, U.; Lepage, O. M.; Gangl, M.; Hilalret, S.; Remandet,

- B.; Meot, F.; Penarier, G.; Segard, E.; Cortez, P.; Jorgensen, C.; Steinberg, R. Development of an equine groove model to induce metacarpophalangeal osteoarthritis: a pilot study on 6 horses. *PLoS One*. **2015**, *10*, e0115089.
102. Carlson, C. S.; Loeser, R. F.; Jayo, M. J.; Weaver, D. S.; Adams, M. R.; Jerome, C. P. Osteoarthritis in cynomolgus macaques: a primate model of naturally occurring disease. *J Orthop Res*. **1994**, *12*, 331-339.
103. Macrini, T. E.; Coan, H. B.; Levine, S. M.; Lerma, T.; Saks, C. D.; Araujo, D. J.; Bredbenner, T. L.; Coutts, R. D.; Nicoletta, D. P.; Havill, L. M. Reproductive status and sex show strong effects on knee OA in a baboon model. *Osteoarthritis Cartilage*. **2013**, *21*, 839-848.
104. Carlson, C. S.; Loeser, R. F.; Purser, C. B.; Gardin, J. F.; Jerome, C. P. Osteoarthritis in cynomolgus macaques. III: Effects of age, gender, and subchondral bone thickness on the severity of disease. *J Bone Miner Res*. **1996**, *11*, 1209-1217.
105. Black, A.; Lane, M. A. Nonhuman primate models of skeletal and reproductive aging. *Gerontology*. **2002**, *48*, 72-80.
106. Buckwalter, J. A.; Martin, J. A.; Olmstead, M.; Athanasiou, K. A.; Rosenwasser, M. P.; Mow, V. C. Osteochondral repair of primate knee femoral and patellar articular surfaces: implications for preventing post-traumatic osteoarthritis. *Iowa Orthop J*. **2003**, *23*, 66-74.
107. Zhou, L.; Gjvm, V. O.; Malda, J.; Stoddart, M. J.; Lai, Y.; Richards, R. G.; Ki-Wai Ho, K.; Qin, L. Innovative tissue-engineered strategies for osteochondral defect repair and regeneration: current progress and challenges. *Adv Healthc Mater*. **2020**, e2001008.
108. Wesdorp, M. A.; Capar, S.; Bastiaansen-Jenniskens, Y. M.; Kops, N.; Creemers, L. B.; Verhaar, J. A. N.; Van Osch, G.; Wei, W. Intra-articular administration of triamcinolone acetonide in a murine cartilage defect model reduces inflammation but inhibits endogenous cartilage repair. *Am J Sports Med*. **2022**, *50*, 1668-1678.
109. Marycz, K.; Smieszek, A.; Targonska, S.; Walsh, S. A.; Szustakiewicz, K.; Wiglusz, R. J. Three dimensional (3D) printed polylactic acid with nano-hydroxyapatite doped with europium(III) ions (nHAp/PLLA@Eu(3+)) composite for osteochondral defect regeneration and theranostics. *Mater Sci Eng C Mater Biol Appl*. **2020**, *110*, 110634.
110. Mendes, L. F.; Katagiri, H.; Tam, W. L.; Chai, Y. C.; Geris, L.; Roberts, S. J.; Luyten, F. P. Advancing osteochondral tissue engineering: bone morphogenetic protein, transforming growth factor, and fibroblast growth factor signaling drive ordered differentiation of periosteal cells resulting in stable cartilage and bone formation in vivo. *Stem Cell Res Ther*. **2018**, *9*, 42.
111. Li, X.; Guo, W.; Zha, K.; Jing, X.; Wang, M.; Zhang, Y.; Hao, C.; Gao, S.; Chen, M.; Yuan, Z.; Wang, Z.; Zhang, X.; Shen, S.; Li, H.; Zhang, B.; Xian, H.; Zhang, Y.; Sui, X.; Qin, L.; Peng, J.; Liu, S.; Lu, S.; Guo, Q. Enrichment of CD146(+) adipose-derived stem cells in combination with articular cartilage extracellular matrix scaffold promotes cartilage regeneration. *Theranostics*. **2019**, *9*, 5105-5121.
112. Ji, X.; Shao, H.; Li, X.; Ullah, M. W.; Luo, G.; Xu, Z.; Ma, L.; He, X.; Lei, Z.; Li, Q.; Jiang, X.; Yang, G.; Zhang, Y. Injectable immunomodulation-based porous chitosan microspheres/HPCH hydrogel composites as a controlled drug delivery system for osteochondral regeneration. *Biomaterials*. **2022**, *285*, 121530.
113. Kim, H. S.; Mandakhbayar, N.; Kim, H. W.; Leong, K. W.; Yoo, H. S. Protein-reactive nanofibrils decorated with cartilage-derived decellularized extracellular matrix for osteochondral defects. *Biomaterials*. **2021**, *269*, 120214.
114. Lin, D.; Cai, B.; Wang, L.; Cai, L.; Wang, Z.; Xie, J.; Lv, Q. X.; Yuan, Y.; Liu, C.; Shen, S. G. A viscoelastic PEGylated poly(glycerol sebacate)-based bilayer scaffold for cartilage regeneration in full-thickness osteochondral defect. *Biomaterials*. **2020**, *253*, 120095.
115. Yang, M.; Zhang, Z. C.; Yuan, F. Z.; Deng, R. H.; Yan, X.; Mao, F. B.; Chen, Y. R.; Lu, H.; Yu, J. K. An immunomodulatory polypeptide hydrogel for osteochondral defect repair. *Bioact Mater*. **2023**, *19*, 678-689.
116. Qi, Y.; Zhang, W.; Li, G.; Niu, L.; Zhang, Y.; Tang, R.; Feng, G. An oriented-collagen scaffold including Wnt5a promotes osteochondral regeneration and cartilage interface integration in a rabbit model. *FASEB J*. **2020**, *34*, 11115-11132.
117. Ye, W.; Yang, Z.; Cao, F.; Li, H.; Zhao, T.; Zhang, H.; Zhang, Z.; Yang, S.; Zhu, J.; Liu, Z.; Zheng, J.; Liu, H.; Ma, G.; Guo, Q.; Wang, X. Articular cartilage reconstruction with TGF- β 1-simulating self-assembling peptide hydrogel-based composite scaffold. *Acta Biomater*. **2022**, *146*, 94-106.
118. Wu, H.; Shang, Y.; Sun, W.; Ouyang, X.; Zhou, W.; Lu, J.; Yang, S.; Wei, W.; Yao, X.; Wang, X.; Zhang, X.; Chen, Y.; He, Q.; Yang, Z.; Ouyang, H. Seamless and early gap healing of osteochondral defects by autologous mosaicplasty combined with bioactive supramolecular nanofiber-enabled gelatin methacryloyl (BSN-GelMA) hydrogel. *Bioact Mater*. **2023**, *19*, 88-102.
119. Hong, Y.; Han, Y.; Wu, J.; Zhao, X.; Cheng, J.; Gao, G.; Qian, Q.; Wang, X.; Cai, W.; Zreiqat, H.; Feng, D.; Xu, J.; Cui, D. Chitosan modified Fe(3)O(4)/KGN self-assembled nanopores for osteochondral MR diagnose and regeneration. *Theranostics*. **2020**, *10*, 5565-5577.
120. Sun, J.; Lyu, J.; Xing, F.; Chen, R.; Duan, X.; Xiang, Z. A biphasic, demineralized, and Decellularized allograft bone-hydrogel scaffold with a cell-based BMP-7 delivery system for osteochondral defect regeneration. *J Biomed Mater Res A*. **2020**, *108*, 1909-1921.
121. Baba, R.; Onodera, T.; Matsuoka, M.; Hontani, K.; Joutoku, Z.; Matsubara, S.; Homan, K.; Iwasaki, N. Bone marrow stimulation technique augmented by an ultrapurified alginate gel enhances cartilage repair in a canine model. *Am J Sports Med*. **2018**, *46*, 1970-1979.
122. Onodera, T.; Baba, R.; Kasahara, Y.; Tsuda, T.; Iwasaki, N. Therapeutic effects and adaptive limits of an acellular technique by ultrapurified alginate (UPAL) gel implantation in canine osteochondral defect models. *Regen Ther*. **2020**, *14*, 154-159.
123. Ryu, J.; Brittberg, M.; Nam, B.; Chae, J.; Kim, M.; Colon Iban, Y.; Magneli, M.; Takahashi, E.; Khurana, B.; Bragdon, C. R. Evaluation of three-dimensional bioprinted human cartilage powder combined with micronized subcutaneous adipose tissues for the repair of osteochondral defects in beagle dogs. *Int J Mol Sci*. **2022**, *23*, 2743.
124. Stefani, R. M.; Lee, A. J.; Tan, A. R.; Halder, S. S.; Hu, Y.; Guo, X. E.; Stoker, A. M.; Ateshian, G. A.; Marra, K. G.; Cook, J. L.; Hung, C. T. Sustained low-dose dexamethasone delivery via a PLGA microsphere-embedded agarose implant for enhanced osteochondral repair. *Acta Biomater*. **2020**, *102*, 326-340.
125. Yan, W.; Xu, X.; Xu, Q.; Sun, Z.; Lv, Z.; Wu, R.; Yan, W.; Jiang, Q.; Shi, D. An injectable hydrogel scaffold with kartogenin-encapsulated nanoparticles for porcine cartilage regeneration: a 12-month follow-up study. *Am J Sports Med*. **2020**, *48*, 3233-3244.
126. Lin, C. C.; Chu, C. J.; Chou, P. H.; Liang, C. H.; Liang, P. I.; Chang, N. J. Beneficial therapeutic approach of acellular PLGA implants coupled with rehabilitation exercise for osteochondral repair: a proof of concept study in a minipig model. *Am J Sports Med*. **2020**, *48*, 2796-2807.
127. Steele, J. A. M.; Moore, A. C.; St-Pierre, J. P.; McCullen, S. D.; Gormley, A. J.; Horgan, C. C.; Black, C. R.; Meinert, C.; Klein, T.; Saifzadeh, S.; Steck, R.; Ren, J.; Woodruff, M. A.; Stevens, M. M. In

Animal models for biomaterial-assisted osteochondral repair

- vitro and in vivo investigation of a zonal microstructured scaffold for osteochondral defect repair. *Biomaterials*. **2022**, *286*, 121548.
128. Asen, A. K.; Goebel, L.; Rey-Rico, A.; Sohler, J.; Zurakowski, D.; Cucchiari, M.; Madry, H. Sustained spatiotemporal release of TGF- β 1 confers enhanced very early chondrogenic differentiation during osteochondral repair in specific topographic patterns. *FASEB J*. **2018**, *32*, 5298-5311.
 129. Huang, Y.; Fan, H.; Gong, X.; Yang, L.; Wang, F. Scaffold with natural calcified cartilage zone for osteochondral defect repair in minipigs. *Am J Sports Med*. **2021**, *49*, 1883-1891.
 130. Bozkurt, M.; Aşık, M. D.; Gürsoy, S.; Türk, M.; Karahan, S.; Gümüşkaya, B.; Akkaya, M.; Şimşek, M. E.; Cay, N.; Doğan, M. Autologous stem cell-derived chondrocyte implantation with bio-targeted microspheres for the treatment of osteochondral defects. *J Orthop Surg Res*. **2019**, *14*, 394.
 131. Vukasovic, A.; Asnaghi, M. A.; Kostesic, P.; Quasnicka, H.; Cozzolino, C.; Pusic, M.; Hails, L.; Trainor, N.; Krause, C.; Figallo, E.; Filardo, G.; Kon, E.; Wixmertens, A.; Maticic, D.; Pellegrini, G.; Kafienah, W.; Hudetz, D.; Smith, T.; Martin, I.; Ivkovic, A.; Wendt, D. Bioreactor-manufactured cartilage grafts repair acute and chronic osteochondral defects in large animal studies. *Cell Prolif*. **2019**, *52*, e12653.
 132. Tamaddon, M.; Blunn, G.; Tan, R.; Yang, P.; Sun, X.; Chen, S. M.; Luo, J.; Liu, Z.; Wang, L.; Li, D.; Donate, R.; Monzón, M.; Liu, C. In vivo evaluation of additively manufactured multi-layered scaffold for the repair of large osteochondral defects. *Biores Manuf*. **2022**, *5*, 481-496.
 133. Favreau, H.; Pijnenburg, L.; Seitlinger, J.; Fioretti, F.; Keller, L.; Scipioni, D.; Adriaensen, H.; Kuchler-Bopp, S.; Ehlinger, M.; Mainard, D.; Rosset, P.; Hua, G.; Gentile, L.; Benkirane-Jessel, N. Osteochondral repair combining therapeutics implant with mesenchymal stem cells spheroids. *Nanomedicine*. **2020**, *29*, 102253.
 134. Critchley, S.; Sheehy, E. J.; Cunniffe, G.; Diaz-Payno, P.; Carroll, S. F.; Jeon, O.; Alsberg, E.; Brama, P. A. J.; Kelly, D. J. 3D printing of fibre-reinforced cartilaginous templates for the regeneration of osteochondral defects. *Acta Biomater*. **2020**, *113*, 130-143.
 135. Jia, S.; Wang, J.; Zhang, T.; Pan, W.; Li, Z.; He, X.; Yang, C.; Wu, Q.; Sun, W.; Xiong, Z.; Hao, D. Multilayered scaffold with a compact interfacial layer enhances osteochondral defect repair. *ACS Appl Mater Interfaces*. **2018**, *10*, 20296-20305.
 136. Burdis, R.; Chariyev-Prinz, F.; Browe, D. C.; Freeman, F. E.; Nulty, J.; McDonnell, E. E.; Eichholz, K. F.; Wang, B.; Brama, P.; Kelly, D. J. Spatial patterning of phenotypically distinct microtissues to engineer osteochondral grafts for biological joint resurfacing. *Biomaterials*. **2022**, *289*, 121750.
 137. Cunniffe, G. M.; Díaz-Payno, P. J.; Sheehy, E. J.; Critchley, S. E.; Almeida, H. V.; Pitacco, P.; Carroll, S. F.; Mahon, O. R.; Dunne, A.; Levingstone, T. J.; Moran, C. J.; Brady, R. T.; O'Brien, F. J.; Brama, P. A. J.; Kelly, D. J. Tissue-specific extracellular matrix scaffolds for the regeneration of spatially complex musculoskeletal tissues. *Biomaterials*. **2019**, *188*, 63-73.
 138. Korshagen, N. M.; Brommer, H.; Hermsen, G.; Plomp, S. G. M.; Melsom, G.; Coeleveld, K.; Mastbergen, S. C.; Weinans, H.; van Buul, W.; van Weeren, P. R. A short-term evaluation of a thermoplastic polyurethane implant for osteochondral defect repair in an equine model. *Vet J*. **2019**, *251*, 105340.
 139. Mancini, I. A. D.; Schmidt, S.; Brommer, H.; Pouran, B.; Schäfer, S.; Tessmar, J.; Mensinga, A.; van Rijen, M. H. P.; Groll, J.; Blunk, T.; Levato, R.; Malda, J.; van Weeren, P. R. A composite hydrogel-3D printed thermoplast osteochondral anchor as example for a zonal approach to cartilage repair: in vivo performance in a long-term equine model. *Biofabrication*. **2020**, *12*, 035028.
 140. Murata, D.; Ishikawa, S.; Sunaga, T.; Saito, Y.; Sogawa, T.; Nakayama, K.; Hobo, S.; Hatazoe, T. Osteochondral regeneration of the femoral medial condyle by using a scaffold-free 3D construct of synovial membrane-derived mesenchymal stem cells in horses. *BMC Vet Res*. **2022**, *18*, 53.
 141. Zanutto, G. M.; Liesbeny, P.; Barrett, M.; Zlotnick, H.; Frank, E.; Grodzinsky, A. J.; Frisbie, D. D. Microfracture augmentation with trypsin pretreatment and growth factor-functionalized self-assembling peptide hydrogel scaffold in an equine model. *Am J Sports Med*. **2021**, *49*, 2498-2508.
 142. Park, D. Y.; Min, B. H.; Park, S. R.; Oh, H. J.; Truong, M. D.; Kim, M.; Choi, J. Y.; Park, I. S.; Choi, B. H. Engineered cartilage utilizing fetal cartilage-derived progenitor cells for cartilage repair. *Sci Rep*. **2020**, *10*, 5722.
 143. Jiang, L.; Ma, A.; Song, L.; Hu, Y.; Dun, H.; Daloz, P.; Yu, Y.; Jiang, J.; Zafarullah, M.; Chen, H. Cartilage regeneration by selected chondrogenic clonal mesenchymal stem cells in the collagenase-induced monkey osteoarthritis model. *J Tissue Eng Regen Med*. **2014**, *8*, 896-905.
 144. Ma, A.; Jiang, L.; Song, L.; Hu, Y.; Dun, H.; Daloz, P.; Yu, Y.; Jiang, J.; Zafarullah, M.; Chen, H. Reconstruction of cartilage with clonal mesenchymal stem cell-acellular dermal matrix in cartilage defect model in nonhuman primates. *Int Immunopharmacol*. **2013**, *16*, 399-408.
 145. Maglio, M.; Brogini, S.; Pagani, S.; Giavaresi, G.; Tschon, M. Current trends in the evaluation of osteochondral lesion treatments: histology, histomorphometry, and biomechanics in preclinical models. *Biomed Res Int*. **2019**, *2019*, 4040236.
 146. Yin, H.; Wang, Y.; Sun, X.; Cui, G.; Sun, Z.; Chen, P.; Xu, Y.; Yuan, X.; Meng, H.; Xu, W.; Wang, A.; Guo, Q.; Lu, S.; Peng, J. Functional tissue-engineered microtissue derived from cartilage extracellular matrix for articular cartilage regeneration. *Acta Biomater*. **2018**, *77*, 127-141.
 147. Martin-Hernandez, C.; Cebamanos-Celma, J.; Molina-Ros, A.; Ballester-Jimenez, J. J.; Ballester-Soleda, J. Regenerated cartilage produced by autogenous periosteal grafts: a histologic and mechanical study in rabbits under the influence of continuous passive motion. *Arthroscopy*. **2010**, *26*, 76-83.
 148. Filardo, G.; Perdida, F.; Gelinsky, M.; Despang, F.; Fini, M.; Marcacci, M.; Parrilli, A. P.; Roffi, A.; Salamanna, F.; Sartori, M.; Schütz, K.; Kon, E. Novel alginate biphasic scaffold for osteochondral regeneration: an in vivo evaluation in rabbit and sheep models. *J Mater Sci Mater Med*. **2018**, *29*, 74.
 149. Jansen, E. J.; Pieper, J.; Gijbels, M. J.; Guldmond, N. A.; Riesle, J.; Van Rhijn, L. W.; Bulstra, S. K.; Kuijjer, R. PEOT/PBT based scaffolds with low mechanical properties improve cartilage repair tissue formation in osteochondral defects. *J Biomed Mater Res A*. **2009**, *89*, 444-452.

Received: November 11, 2022

Revised: November 26, 2022

Accepted: December 10, 2022

Available online: December 28, 2022